

# Pre-trained Model Guided Mixture Knowledge Distillation for Adversarial Federated Learning

Yu Qiao<sup>1</sup>, Huy Q. Le<sup>1</sup>, Apurba Adhikary<sup>1</sup>, Choong Seon Hong<sup>1\*</sup>

<sup>1</sup>School of Computing, Kyung Hee University, Yongin-si 17104, Republic of Korea

<sup>1</sup>{qiaoyu, quanghuy69, apurba, cshong}@khu.ac.kr

## Abstract

This paper aims to improve the robustness of a small global model while maintaining clean accuracy under adversarial attacks and non-IID challenges in federated learning. By leveraging the concise knowledge embedded in the class probabilities from a pre-trained model for both clean and adversarial image classification, we propose a Pre-trained Model-guided Adversarial Federated Learning (PM-AFL) training paradigm. This paradigm integrates vanilla mixture and adversarial mixture knowledge distillation to effectively balance accuracy and robustness while promoting local models to learn from diverse data. Specifically, for clean accuracy, we adopt a dual distillation strategy where the class probabilities of randomly paired images and their blended versions are aligned between the teacher model and the local models. For adversarial robustness, we use a similar distillation approach but replace clean samples on the local side with adversarial examples. Moreover, considering the bias between local and global models, we also incorporate a consistency regularization term to ensure that local adversarial predictions stay aligned with their corresponding global clean ones. These strategies collectively enable local models to absorb diverse knowledge from the teacher model while maintaining close alignment with the global model, thereby mitigating overfitting to local optima and enhancing the generalization of the global model. Experiments demonstrate that the PM-AFL-based paradigm outperforms other methods that integrate defense strategies by a notable margin.

## 1. Introduction

Federated learning (FL) has emerged as an advanced paradigm for training machine learning models in a decentralized manner, where multiple clients collaboratively build a shared global model while keeping their private data confidential [33]. This approach is particularly relevant in scenarios involving sensitive or personal information such

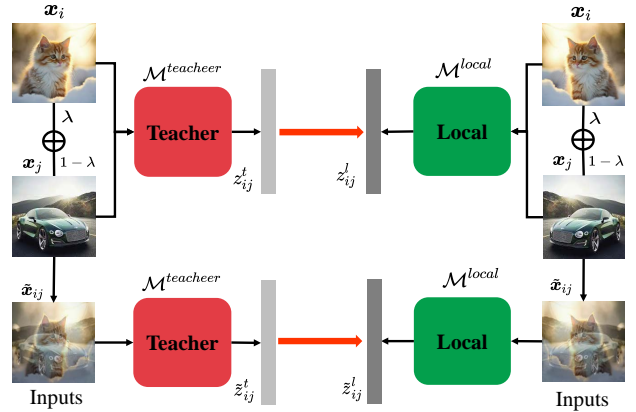


Figure 1. Illustration of vanilla mixture KD in PM-AFL++. Each local model is guided to learn from the teacher model’s predictions on random image pairs and their blended counterparts, enhancing its abilities to learn from diverse data.

as healthcare [2], finance [30], and social media [41], as it preserves data privacy and security. However, despite its advantages, FL faces several challenges, notably the non-IID (non-independent and identically distributed) data issue, which can hinder model performance and generalization [38].

Recently, similar to centralized machine learning, researchers have also found that FL models are vulnerable to adversarial examples (AEs) [12, 43], which are images modified with carefully crafted, imperceptible perturbations that can mislead model predictions. These AE attacks can pose a significant threat to the secure deployment of FL models in real-world applications (i.e., autonomous driving) [18, 65]. Furthermore, the inherent non-IID data distribution across clients may exacerbate the problem, making it even more challenging to achieve both adversarial robustness and high natural accuracy [39, 61]. To address these concerns, researchers have explored various strategies. One approach is robustness sharing [18, 65], where adversarial training (AT) is conducted at high-resource clients, and the resulting robustness is shared with low-resource clients. Another line of research focuses on logit adjust-

ment [7, 37, 61], which involves reweighting the logit of adversarially trained models to improve their robustness. Additionally, feature sharing [39, 40] techniques are employed to boost the resilience of FL models against attacks by contrasting adversarial features with clean ones. Nonetheless, these methods share a common weakness: they require local clients to train their models from scratch, resulting in excessive computational and communication demands, particularly when dealing with large-scale models.

Moreover, previous research on adversarial knowledge distillation (KD) [5, 11, 17, 64] has shown that a robust teacher model can simultaneously produce student models with higher robust accuracy and natural accuracy. However, whether this observation holds in the context of adversarial federated learning remains an open question. To address this, we conduct a toy example, as shown in Table 1. We begin by exploring vanilla KD, which relies solely on clean samples for distillation. The results indicate that while a significant portion of clean performance can be inherited, the transfer of robust behavior is limited. Next, we examine adversarial KD, which utilizes AEs during distillation. We observe that, compared to vanilla KD, adversarial KD exhibits improved robustness but compromises clean accuracy. Interestingly, this observation somewhat differs from prior findings, as we note that although adversarial KD inherits both clean and robust accuracy to some extent, its clean accuracy is significantly lower than that of vanilla KD (45.64% vs. 56.78%). This inspires us to leverage the advantages of both vanilla KD and adversarial KD to strike a balance between clean accuracy and robust accuracy. The results of PM-AFL (Pre-trained Model-guided Adversarial Federated Learning) further support this approach, demonstrating that significantly fewer parameters need to be communicated per round (0.3M vs. 11.69M) while maintaining high accuracy, outperforming models trained from scratch.

However, given that data imbalance and non-IID distributions are common challenges in FL, we further design a novel lightweight framework called PM-AFL++. PM-AFL++ leverages both natural and virtual samples to perform vanilla mixture KD and adversarial mixture KD, effectively balancing accuracy and robustness while encouraging local models to enhance data diversity and improve generalization. As shown in Figure 1, we demonstrate the vanilla mixture KD process (i.e., distillation on clean samples) as an example. First, the original image  $x_i$  and a random image  $x_j$  are linearly interpolated with a mixing coefficient  $\lambda$  to generate a mixed image  $\tilde{x}_{ij}$ . Next, we compute the class probabilities for these input images, where  $z_{ij}^t$  and  $z_{ij}^l$  are obtained by  $\lambda\mathcal{M}^{teacher}(x_i) + (1-\lambda)\mathcal{M}^{teacher}(x_j)$  and  $\lambda\mathcal{M}^{local}(x_i) + (1-\lambda)\mathcal{M}^{local}(x_j)$ , respectively. Similarly,  $\tilde{z}_{ij}^t$  and  $\tilde{z}_{ij}^l$  are derived from  $\mathcal{M}^{teacher}(\tilde{x}_{ij})$  and  $\mathcal{M}^{local}(\tilde{x}_{ij})$ , respectively. Note that although the soft label  $\tilde{z}_{ij}^t$  and  $\tilde{z}_{ij}^l$  generated from the teacher may indicate in-

correct classes, the relative probability distribution still provides valuable information about the similarities between classes [53]. Therefore, as  $z_{ij}^t$  incorporates information from two classes and  $\tilde{z}_{ij}^t$  represents an augmented result, both can be regarded as pseudo-ground-truth labels that provide comprehensive knowledge and promote simple linear behavior in-between training examples, effectively guiding each local model to learn smoother and more robust representations [8, 57]. On the other hand, to enhance adversarial robustness, we perform a distillation process similar to the one above, but replace the input samples on the local side with AEs. Moreover, given that the update direction of local models may differ from that of the global model, we further introduce a consistency regularization term that constrains the local updates to remain close to their global counterparts. Together, these strategies establish PM-AFL++ as a competitive approach, achieving higher clean and robust accuracy while ensuring privacy protection, without requiring additional information exchange between local clients and the server. The main contributions are summarized below:

- We address the challenges of adversarial attacks and label non-IID scenarios in FL, recognizing that training robust federated models from scratch is both computationally intensive and communication-heavy. Moreover, we find that neither vanilla KD nor adversarial KD alone can effectively inherit both accuracy and robustness from the teacher model.
- We propose a PM-AFL-guided training paradigm that leverages a unified mixture dual-KD framework to enable effective knowledge transfer between a teacher model and local models. Moreover, we introduce a consistency term to align local updates with global updates, mitigating the challenges of data heterogeneity.
- We conduct extensive experiments on popular benchmark datasets, along with ablation studies, to validate the effectiveness of the PM-AFL-guided training paradigm and demonstrate the indispensability of each module.

## 2. Related Work

### 2.1. Federated Learning

To address privacy concerns, FL is developed to train machine learning models in a distributed environment without requiring local data sharing. The pioneering approach, FedAvg [33], trains a global model by aggregating model updates from multiple clients with non-IID data distributions. Since then, various existing methods have been dedicated to further improving the performance of FedAvg from different perspectives. For example, FedProx [28], FedAvgM [20], and pFedME [44] concentrate on aligning local models with the global model to ensure model update consistency. Besides, MOON [27], FedProto [45], and FPL [22] aim to improve feature alignment between local

Setup	Param.↓	Rounds↓	Acc.↑	Rob.↑
Training from scratch	11.69 M	200	28.82	17.22
Vanilla KD	0.30 M	150	56.78	3.20
Adversarial KD	0.30 M	150	45.64	15.82
PM-AFL	0.30 M	150	45.76	18.74
PM-AFL++	0.30 M	150	47.88	20.22

Table 1. Compared to training from scratch, PM-AFL++ requires fewer communication rounds and fewer learnable parameters while achieving higher performance. Experiments are conducted on CIFAR-10 with a Dirichlet [4] parameter of 0.1. “Acc.” denotes clean accuracy (%) and “Rob.” denotes robust accuracy (%) against AutoAttack [9].

and global models by emphasizing feature consistency. Additionally, FedLC [60] and FedCSD [51] focus on adjusting the alignment between local and global predictions from a logit perspective. Moreover, FedGen [63] and DFRD [47] employ data-free KD techniques to address heterogeneity in FL. Similarly, FedAF [49] replaces the traditional aggregate-then-adapt FL approach with an aggregation-free strategy. The major limitation of these methods is that they are designed for conventional FL scenarios where adversarial attacks are not considered, resulting in FL models that lack robustness against such attacks.

## 2.2. Knowledge Distillation

By transferring concise knowledge from a high-performance teacher model to a smaller student model, KD enables the student to achieve near-teacher performance with limited computing resources. The pioneering strategy [17] utilizes response-based knowledge [17, 42] such as logit output as the information carrier for the distillation process. Additionally, researchers have explored various types of knowledge for intermediate-level guidance to better leverage additional supervision from the teacher model, including feature-based [15, 52] and relation-based distillation [35, 50]. In FL, studies [29, 31] suggest treating the ensemble of local models as the teacher and the global model as the student, with the global model trained to match the averaged outputs of the local models. Moreover, recent studies have introduced AD [10, 11], which focuses on enhancing model robustness by incorporating AEs into the distillation process. For example, FatCC [39] aligns adversarial and clean features between the local and global models. DBFAT [61] constrains the global and local models’ logits, with the local model’s logits being derived from AEs. However, these methods require AT of models from scratch, which is computationally and communicatively demanding, especially with large-scale models. In contrast, PM-AFL++ proposes a lightweight framework by utilizing a well-trained robust teacher model to transfer both its accuracy and robustness to the local lightweight models.

## 2.3. Adversarial Attack and Defense

Neural network models have been found to be vulnerable to AEs that are imperceptible to human vision [43]. This vulnerability, first identified by [43], raises significant security concerns when deploying these models in real-world applications, such as autonomous driving scenarios [46]. Adversarial attacks can be classified into white-box and black-box attacks, depending on the attacker’s level of access to the model’s internal information [36]. In white-box attacks, the attacker has full access to the model’s details, while in black-box attacks, the attacker does not have access to such information. The fast gradient sign method (FGSM) [12] is a single-step technique for generating AEs. In contrast, projected gradient descent (PGD) [32] and basic iterative method (BIM) [25] are iterative extensions of FGSM that use multiple steps to craft AEs. Additionally, several more advanced attack algorithms have been developed, such as the Square attack [1], Carlini and Wagner (C&W) attack [6], and AutoAttack (AA) [9]. Another line of work focuses on finding a single universal attack perturbation (UAP) [34] that can cause the model to misclassify all images. To defend against adversarial attacks, AT is widely regarded as one of the most effective strategies [58]. Recently, several studies [7, 18, 37, 65] have implemented AT in FL to develop a robust global model. Orthogonal to these works, this paper explores a lightweight yet robust FL framework by utilizing an image augmentation-based dual-KD process.

## 3. Methodology

### 3.1. Overview

Following the conventional federated setting [33, 54], we assume there are  $N$  clients, each with a private dataset  $\mathcal{D}_i = \{\mathbf{x}_i, y_i\}$  of size  $D_i$ . In the label non-IID setting, each client’s sample proportions for each label follow a Dirichlet distribution [4]. This results in varying marginal distributions  $P(y)$  across clients, while the conditional distribution  $P_i(y|x) = P_j(y|x)$  remains the same for all clients  $i$  and  $j$ . Besides, all clients share the same model architecture, with an edge server coordinating the collaborative training, and each client has access to a well-trained, robust teacher model. Under these conditions, the local training objective for each client can be formulated as follows:

$$\mathcal{L}_i(\omega_i) = -\frac{1}{D_i} \sum_{i \in \mathcal{D}_i} \sum_{j=1}^C \mathbb{1}_{y=j} \log \frac{e^{z_{i,j}}}{\sum_{j=1}^C e^{z_{i,j}}}, \quad (1)$$

where  $z$  denotes the model output, which is then aligned with the output of the teacher model,  $\mathbb{1}(\cdot)$  is the indicator function,  $\omega_i$  represents the model parameters, and  $C$  denotes the number of classes. Then, the global objective is to

aggregate the local loss across distributed clients as follows:

$$\mathcal{L}(\omega) = \sum_{i \in [N]} \frac{D_i}{\sum_{i \in [N]} D_i} \mathcal{L}_i(\omega_i), \quad (2)$$

where  $\omega$  represents the global model parameters, and  $[N]$  denotes the set of distributed clients with  $[N] = \{1, \dots, N\}$ . The goal of optimization is to enhance the robustness of the global model by distilling knowledge from a well-trained teacher model to local models during local training, thereby improving the global model after each global communication round.

### 3.2. Adversarial Attacks Meet Federated Learning

Adversarial attacks can easily mislead a model by introducing carefully crafted, imperceptible perturbations, resulting in incorrect predictions [43]. For any given client, the classification layer of the model is represented as  $\phi_i(\mathbf{x}_i) : \mathbb{R}^{h \times w \times c} \rightarrow [C]$ , mapping the input image  $\mathbf{x}_i$  to a discrete set of labels  $[C]$ , where  $h$ ,  $w$ , and  $c$  denote the height, width, and number of channels of the image, respectively. To find a well-crafted perturbation  $\delta \in \mathbb{R}^{h \times w \times c}$  that causes  $\phi(\mathbf{x}_i + \delta) \neq \phi(\mathbf{x}_i)$ , we use the PGD attack to iteratively generate the AEs as follows:

$$\mathbf{x}_i^{t+1} = \Pi_{\mathbf{x}_i + \delta}(\mathbf{x}_i^t + \alpha \text{sign}(\nabla_{\mathbf{x}_i} \mathcal{L}_i(\omega_i; \mathbf{x}_i^t, y_i))), \quad (3)$$

where  $\alpha$  represents the step size,  $\mathbf{x}_i^t$  is the AE generated at the  $t$ -th step,  $\Pi_{\mathbf{x}_i + \delta}(\cdot)$  projects the perturbed input into the feasible region  $\mathbf{x}_i + \delta$ , and  $\text{sign}(\cdot)$  denotes the sign function. Meanwhile, to ensure that the perturbation  $\delta$  is imperceptible to the human vision, it is constrained by an upper bound  $\epsilon$ . Thus, during each iteration of the PGD attack, the optimal perturbation  $\delta^*$  is found by maximizing the local objective in Eq. 1:

$$\delta^* = \arg \max_{\|\delta\|_\infty \leq \epsilon} \mathcal{L}_i(\omega_i; \mathbf{x}_i + \delta, y_i), \quad (4)$$

where  $\delta^*$  denotes the obtained perturbation after the predefined number of iterations of PGD attack algorithm, and the AEs  $\mathbf{x}_i^{adv}$  are then derived as:

$$\mathbf{x}_i^{adv} = \mathbf{x}_i + \delta^*. \quad (5)$$

**Motivation.** To defend against such attacks, a common practice in existing work [7, 18, 39, 61] is to integrate AT into the local training stage of the federated training process, given that AT is a widely recognized and established approach [3]. In particular, the AEs derived in Eq. 5 are used as new inputs for each local training process. For any given client, by minimizing the loss with these AEs, each local model is expected to be more robust to such attacks, as formulated below:

$$\min_{\omega} \mathbb{E}_{(\mathbf{x}_i^{adv}, y_i) \sim \mathcal{D}_i} \mathcal{L}_i(\omega_i; \mathbf{x}_i^{adv}, y_i). \quad (6)$$

However, as demonstrated in Table 1, training a robust model from scratch using pure AT is resource-intensive. In contrast, the KD-based approach shows promising results with fewer resources and higher performance. This motivates us to explore how to conduct KD to develop a robust and generalizable global model with lower resource demands.

### 3.3. Knowledge Distillation in Federated Learning

To improve the performance of smaller local models, KD is a natural choice, enabling the transfer of a large teacher model’s performance to resource-constrained local models. In this paper, we define vanilla KD as distillation performed only on clean samples between the teacher model and local models, while adversarial KD involves aligning the knowledge of local models on AEs with the teacher model’s knowledge of clean samples.

**Vanilla Knowledge Distillation.** The output behavior of the small student model can be encouraged to mimic that of the teacher model through the teacher-student KD paradigm, thereby enabling the student to achieve performance close to the teacher model [17]. For any arbitrary client, this distillation process is optimized by solving the following minimization problem:

$$\min_{\omega} \mathbb{E}_{\mathbf{x} \sim \mathcal{D}} [\mathcal{L}_{vkd}(\mathcal{M}_{\omega}^{local}(\mathbf{x}), \mathcal{M}^{teacher}(\mathbf{x}))], \quad (7)$$

where  $\mathcal{L}_{vkd}$  denotes the vanilla distillation loss function, which encourages the local model’s output logits to align with those of the teacher model,  $\mathcal{M}_{\omega}^{local}(\cdot)$  represents the local model with parameters  $\omega$  to be optimized, and  $\mathcal{M}^{teacher}(\cdot)$  is the teacher model with fixed parameters. Note that in this vanilla KD, both the local model and the teacher model receive clean, unperturbed images as input.

**Adversarial Knowledge Distillation.** To enhance the robustness of student models, we constrain the logits output from robust local models, which take AEs as input, to closely match those from the teacher model fed with the corresponding clean examples. This distillation process can be formulated as follows:

$$\min_{\omega} \mathbb{E}_{\mathbf{x}^{adv}, \mathbf{x} \sim \mathcal{D}} [\mathcal{L}_{akd}(\mathcal{M}_{\omega}^{local}(\mathbf{x}^{adv}), \mathcal{M}^{teacher}(\mathbf{x}))], \quad (8)$$

where  $\mathcal{L}_{akd}$  denotes the adversarial distillation loss function. Note that we adopt KL divergence as the loss function in our method, following the common practice in the KD paradigm.

### 3.4. Federated Mixture Knowledge Distillation

To illustrate how mixture dual-KD is performed among local clients, we detail the process of creating mixture models and conducting mixture dual-KD between the

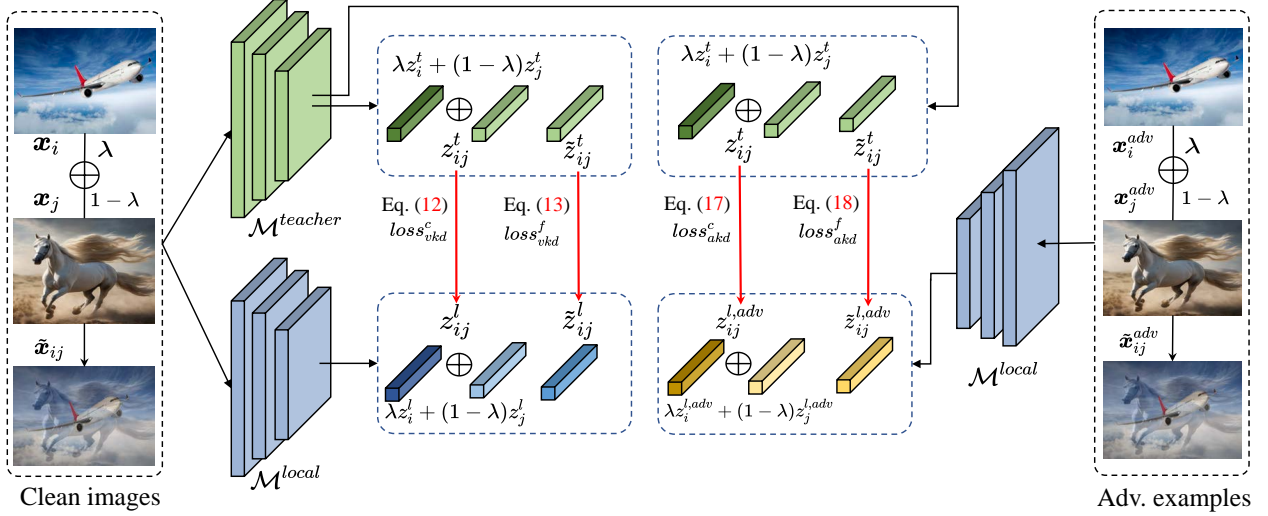


Figure 2. Illustration of the proposed mixture dual-KD of PM-AFL++ framework. We align  $z_{ij}^l$  of the local model with the corresponding  $z_{ij}^t$  to capture diverse class information. Meanwhile, we align  $\tilde{z}_{ij}^l$  with the corresponding  $\tilde{z}_{ij}^t$ , ensuring that the local model inherits the simpler, linear behavior of the teacher’s mixed outputs. We apply a similar strategy for robustness by encouraging the adversarial logits output  $z_{ij}^{l,adv}$  and  $\tilde{z}_{ij}^{l,adv}$  to align with  $\tilde{z}_{ij}^t$  and  $z_{ij}^t$ , respectively.

teacher model and local models, as shown in Figure 2. Additionally, the consistency regularization term is depicted in Figure 3.

**Vanilla Mixture Knowledge Distillation.** Given two different clean images,  $\mathbf{x}_i$  and  $\mathbf{x}_j$ , we blend them using a combination factor  $\lambda$ , which controls the mixing ratio, as follows [57]:

$$\tilde{\mathbf{x}}_{ij} = \lambda \mathbf{x}_i + (1 - \lambda) \mathbf{x}_j \quad (9)$$

where  $\tilde{\mathbf{x}}_{ij}$  is an augmented image, and  $\lambda$  is sampled from  $\text{Beta}(\beta, \beta)$  with  $\beta \in (0, +\infty)$ .

Next, the input images  $\mathbf{x}_i$ ,  $\mathbf{x}_j$ , and the augmented image  $\tilde{\mathbf{x}}_{ij}$  are fed into the teacher model to obtain the corresponding class probabilities (i.e., logits), as follows:

$$\begin{aligned} z_{ij}^t &= \lambda \mathcal{M}^{\text{teacher}}(\mathbf{x}_i) + (1 - \lambda) \mathcal{M}^{\text{teacher}}(\mathbf{x}_j), \\ \tilde{z}_{ij}^t &= \mathcal{M}^{\text{teacher}}(\tilde{\mathbf{x}}_{ij}), \end{aligned} \quad (10)$$

where  $z_{ij}^t$  represents the teacher model’s linearly interpolated class probabilities based on the inputs  $\mathbf{x}_i$  and  $\mathbf{x}_j$ , and  $\tilde{z}_{ij}^t$  denotes the class probabilities for the augmented image  $\tilde{\mathbf{x}}_{ij}$ .

For an arbitrary local client, the input images  $\mathbf{x}_i$ ,  $\mathbf{x}_j$ , and the augmented image  $\tilde{\mathbf{x}}_{ij}$  are similarly fed into each local model to obtain the corresponding class probabilities (i.e., logits), as follows:

$$\begin{aligned} z_{ij}^l &= \lambda \mathcal{M}^{\text{local}}(\mathbf{x}_i) + (1 - \lambda) \mathcal{M}^{\text{local}}(\mathbf{x}_j), \\ \tilde{z}_{ij}^l &= \mathcal{M}^{\text{local}}(\tilde{\mathbf{x}}_{ij}), \end{aligned} \quad (11)$$

where  $z_{ij}^l$  represents the local model’s linearly interpolated class probabilities based on the inputs  $\mathbf{x}_i$  and  $\mathbf{x}_j$ , while  $\tilde{z}_{ij}^l$  denotes the class probabilities of the local model using the augmented image  $\tilde{\mathbf{x}}_{ij}$ .

Since  $z_{ij}^t$  from the teacher model encodes the predictive information from two random input images, it can provide more knowledge to guide the corresponding image  $z_{ij}^l$  from each local model. Therefore, the distillation process is defined as follows:

$$\text{loss}_{vkd}^c = T^2 * KL(p(z_{ij}^t, T), p(z_{ij}^l, T)), \quad (12)$$

where  $T$  is the temperature, introduced to control the influence of soft labels, and  $p_i = \frac{\exp(z_i/T)}{\sum_j \exp(z_j/T)}$ .

Meanwhile, we encourage the class probabilities of augmented image  $\tilde{z}_{ij}^l$  in each local model to align with the corresponding augmented class probability  $\tilde{z}_{ij}^t$  from the teacher model. In other words, since  $\tilde{z}_{ij}^t$  represents an augmented class probability, it enables local models to inherit the capability of favoring simple linear behavior in-between training examples, leading to more robust predictions [57]. We formulate this process as follows:

$$\text{loss}_{vkd}^f = T^2 * KL(p(\tilde{z}_{ij}^t, T), p(\tilde{z}_{ij}^l, T)). \quad (13)$$

Overall, the vanilla mixture KD process, involving both  $\text{loss}_{vkd}^c$  and  $\text{loss}_{vkd}^f$ , encourages the network to produce consistent predictions for the input images  $\mathbf{x}_i$  and  $\mathbf{x}_j$  and their corresponding augmented image  $\tilde{\mathbf{x}}_{ij}$ . This can be expressed as:

$$\text{loss}_{vkd} = \text{loss}_{vkd}^c + \text{loss}_{vkd}^f. \quad (14)$$

**Adversarial Mixture Knowledge Distillation.** To enhance robust generalization, we perform adversarial mixture distillation between the local and teacher models, following a similar approach to vanilla mixture KD.

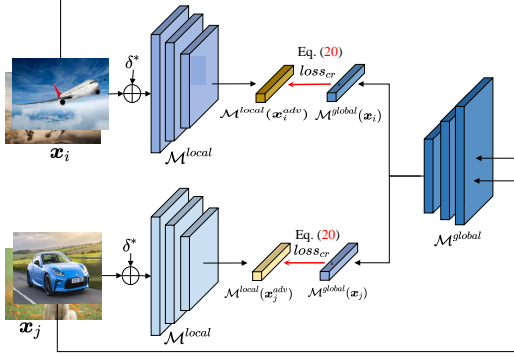


Figure 3. Illustration of the proposed consistency regularization in PM-AFL++ framework. We pull the local updates  $\mathcal{M}^{local}(\mathbf{x}^{adv})$  closer to the global updates  $\mathcal{M}^{global}(\mathbf{x})$ , guiding each local model’s training towards better alignment with the global model.

We first generate AEs,  $\mathbf{x}_i^{adv}$  and  $\mathbf{x}_j^{adv}$  using Eq. 3 with constraints from Eq. 4, and then blend them using a mixing factor  $\lambda$ , as follows [57]:

$$\tilde{\mathbf{x}}_{ij}^{adv} = \lambda \mathbf{x}_i^{adv} + (1 - \lambda) \mathbf{x}_j^{adv}, \quad (15)$$

where  $\tilde{\mathbf{x}}_{ij}^{adv}$  represents the augmented AEs, and  $\lambda$  is sampled from Beta( $\beta, \beta$ ) with  $\beta \in (0, +\infty)$ .

Next, for an arbitrary local client, we feed the input AEs  $\mathbf{x}_i^{adv}$ ,  $\mathbf{x}_j^{adv}$ , and the augmented AE  $\tilde{\mathbf{x}}_{ij}^{adv}$  into the local model to obtain the corresponding class probabilities (logits) as follows:

$$\begin{aligned} z_{ij}^{l,adv} &= \lambda \mathcal{M}^{local}(\mathbf{x}_i^{adv}) + (1 - \lambda) \mathcal{M}^{local}(\mathbf{x}_j^{adv}), \\ \tilde{z}_{ij}^{l,adv} &= \mathcal{M}^{local}(\tilde{\mathbf{x}}_{ij}^{adv}), \end{aligned} \quad (16)$$

where  $z_{ij}^{l,adv}$  represents the local model’s linearly interpolated class probabilities based on the AEs  $\mathbf{x}_i^{adv}$  and  $\mathbf{x}_j^{adv}$ , while  $\tilde{z}_{ij}^{l,adv}$  denotes the class probabilities of the local model using the augmented AEs  $\tilde{\mathbf{x}}_{ij}^{adv}$  as input.

We then align  $z_{ij}^{l,adv}$  from each local model with  $z_{ij}^t$  from the teacher model, which is obtained using Eq. 10. The distillation process can be defined as:

$$loss_{akd}^c = T^2 * KL(p(z_{ij}^t, T), p(z_{ij}^{l,adv}, T)). \quad (17)$$

Meanwhile, we encourage the local model’s class probabilities of augmented AEs  $\tilde{z}_{ij}^{l,adv}$  to align with the corresponding augmented class probabilities  $\tilde{z}_{ij}^t$  from the teacher model, which can be expressed as:

$$loss_{akd}^f = T^2 * KL(p(\tilde{z}_{ij}^t, T), p(\tilde{z}_{ij}^{l,adv}, T)). \quad (18)$$

Overall, the adversarial mixture KD process, which includes both  $loss_{akd}^c$  and  $loss_{akd}^f$ , encourages consistent predictions from the local model for AEs  $\mathbf{x}_i^{adv}$  and  $\mathbf{x}_j^{adv}$ , as well as their corresponding augmented image  $\tilde{\mathbf{x}}_{ij}^{adv}$ . This can be expressed as:

$$loss_{akd} = loss_{akd}^c + loss_{akd}^f. \quad (19)$$

**Consistency Regularization.** Due to the non-IID distribution across clients, the update direction of local models may diverge from that of the global model, potentially leading to misalignment. Therefore, we further introduce a consistency regularization term to pull the local updates closer to the global updates, which is calculated as follows:

$$loss_{cr} = \mathcal{L}_{cr}(z_l^{adv}, z_g), \quad (20)$$

where  $z_l^{adv} = \mathcal{M}^{local}(\mathbf{x}_i^{adv})$  denotes the adversarial logits output from each local model, and  $z_g = \mathcal{M}^{global}(\mathbf{x}_i)$  represents the clean logits output from the global model. We employ MSE loss to define  $loss_{cr}$ , which measure the consistency between local models and the global model.

**Overall Objective Function.** The proposed PM-AFL++ framework consists of three key components. The first component,  $loss_{vkd}$ , facilitates mutual vanilla distillation between local models and the teacher model, enabling the inheritance of clean accuracy. The second component,  $loss_{akd}$ , enhances robustness through mutual adversarial distillation by aligning the logits distribution between clean images and AEs. The third component,  $loss_{cr}$ , ensures that local updates are close to global updates, mitigating the effects of biased updating. By optimizing these components simultaneously, these strategies collectively enable local models to absorb diverse knowledge from the teacher model while maintaining close alignment with the global model, thereby improving the global model’s generalization. Finally, the overall objective function is formulated as follows:

$$loss_{total} = \gamma * loss_{vkd} + (1 - \gamma) * loss_{akd} + loss_{cr}, \quad (21)$$

where  $loss_{total}$  represents the overall local objective for each client during its local training phase, with  $\gamma$  denoting the weight that balances accuracy and robustness. The detailed training process is shown in the Appendix.

## 4. Experiments

### 4.1. Experimental Setup

**Datasets and Baselines.** We conduct experiments on two widely used benchmark datasets: MNIST [26] and CIFAR-10 [24], to verify the effectiveness of the proposed PM-AFL++. Since adversarial federated learning research is still in its early stages with limited established methods, we incorporate four well-established defense methods, including PGD-AT [32], ALP [23], MART [48], and TRADES [59] into the FL framework, and refer to them as FedPGD, FedALP, FedMART, and FedTRADES, respectively. In addition, for a more comprehensive evaluation, we compare PM-AFL++ with three other state-of-the-art federated defense methods such as MixFAT [65], CalFAT [7], and DBFAT [61], as well as FedAvg, which denotes typical federated training without adversarial training process.

Dataset	Method	Clean Acc.	Robust Acc.						# of Comm Rounds	# of Comm Params ( $\times 10^3$ )	
			FGSM	BIM	PGD-40	PGD-100	Square	AA			Avg
CIFAR-10	FedAvg [33]	63.58	3.22	0.00	0.00	0.00	0.36	0.00	0.59	200	11,690
	MixFAT [65]	38.94	22.68	21.24	21.32	21.22	20.48	18.08	20.83	250	11,690
	FedPGD [32]	28.82	19.82	19.50	19.48	19.42	18.36	17.22	18.96	200	11,690
	FedALP [23]	31.54	21.18	20.15	20.10	20.08	18.70	16.86	19.51	200	11,690
	FedMART [48]	35.34	22.67	20.64	20.15	19.93	19.13	17.82	20.05	200	11,690
	FedTRADES [59]	36.00	21.06	19.62	19.64	19.54	19.80	17.32	19.49	230	11,690
	CalFAT [7]	32.24	20.98	19.66	19.68	19.60	18.72	16.98	19.27	200	11,690
	DBFAT [61]	30.82	18.32	18.00	17.92	17.90	17.42	16.64	17.70	200	11,690
	PM-AFL	45.76	24.46	23.96	22.96	22.94	21.26	18.74	22.38	150	320
	PM-AFL++	<b>47.88</b>	<b>26.80</b>	<b>24.62</b>	<b>24.68</b>	<b>24.66</b>	<b>23.20</b>	<b>20.22</b>	<b>24.03</b>	<b>150</b>	<b>320</b>
MNIST	FedAvg [33]	90.54	37.64	0.68	0.00	0.00	0.16	0.00	6.41	160	3,217
	MixFAT [65]	91.30	52.92	48.78	15.24	6.32	0.70	0.04	20.66	160	3,217
	FedPGD [32]	91.54	51.74	52.46	18.06	7.72	0.40	0.06	21.74	160	3,217
	FedALP [23]	94.06	64.62	60.02	29.24	12.18	1.26	0.76	28.01	180	3,217
	FedMART [48]	93.74	61.24	47.52	16.76	7.20	0.76	0.26	22.29	160	3,217
	FedTRADES [59]	94.32	<b>66.26</b>	51.80	17.92	4.46	0.46	0.04	23.49	160	3,217
	CalFAT [7]	93.60	64.48	45.38	14.78	1.68	0.20	0.06	21.09	180	3,217
	DBFAT [61]	93.58	66.14	61.70	37.62	16.82	0.44	0.34	30.51	180	3,217
	PM-AFL	94.53	57.89	72.15	33.41	18.72	17.84	13.66	35.61	100	44
	PM-AFL++	<b>94.68</b>	63.96	<b>77.50</b>	<b>43.10</b>	<b>29.92</b>	<b>27.52</b>	<b>23.62</b>	<b>44.27</b>	<b>100</b>	<b>44</b>

Table 2. Comparison of different methods on benchmark datasets under non-IID data. The best results are in **bold**. PM-AFL++ appears to outperform the baselines, achieving higher accuracy (%) and robustness (%) while requiring significantly fewer communicated parameters.

Note that for comparison, we also present the results of PM-AFL, which incorporates only the single KD process. To evaluate the effectiveness of our proposed method, we utilize six mainstream attack techniques such as FGSM [12], BIM [25], PGD [32], Square [1], and AA [9]. All experimental results are reported based on 5 clients by default.

**Implementation Details.** We adopt CNN models as local models for the MNIST and CIFAR-10 tasks in PM-AFL++. For the teacher model, we utilize the pre-trained WideResNet-34-10 [55] and WideResNet-28-10 [55] for CIFAR-10 and MNIST, respectively. Note that the teacher model is used locally, involves only forward propagation, and is not sent to the server for aggregation. Therefore, no additional communication costs are incurred. For baselines, we adopt ResNet-18 [16] and MobileNet [19] for CIFAR-10 and MNIST, respectively. To simulate non-IID settings, we employ the Dirichlet distribution  $\text{Dir}(a)$  [54], with  $a$  set to 0.1 by default. Following the suggestions in [57], we set  $\lambda = 0.2$  for both MNIST and CIFAR-10 datasets. In addition, following [12], we set the perturbation bound to  $8/255$  and the step size to  $2/255$  for CIFAR-10, while for MNIST, we set the perturbation bound to 0.3 and the step size to 0.01. A detailed setup, including the selection of hyperparameters, is provided in Appendix.

## 4.2. Performance Comparison

**Accuracy Comparison.** We present the performance comparison in Table 2, including clean accuracy and robust accuracy. Clean accuracy is assessed on unperturbed samples, while robust accuracy is evaluated using six metrics:

FGSM, BIM, PGD-40, PGD-100, Square, and AA attacks. To provide a comprehensive evaluation, we also report the average robustness score across these six metrics. Several observations can be drawn from the results. First, adversarial attacks present a significant challenge to federated models. For example, in the CIFAR-10 task, the clean accuracy of FedAvg dramatically declines from 63.58% to an average of merely 0.59% following six different attacks. Second, despite the substantial challenges posed by adversarial attacks, our strategy, PM-AFL++, demonstrates impressive performance on both the CIFAR-10 and MNIST datasets, achieving superior clean accuracy and average robust accuracy compared to all other methods. These observations indicate that PM-AFL++ has a clear advantage in enhancing both model accuracy and robustness under adversarial attacks and non-IID challenges.

**Communication Efficiency.** Given that communication has always been a challenge in FL due to the limitations of existing communication channels, we also report the number of communication rounds required for convergence and the number of parameters communicated per round in Table 2. Notably, it can be observed that the number of parameters communicated per round in PM-AFL++ is significantly lower than that of other baselines. Moreover, PM-AFL++ requires the fewest communication rounds to complete the global model training. For example, in the MNIST results, with approximately 73 times fewer communication parameters per round and 1.6 times fewer communication rounds, PM-AFL++ achieves a clean accuracy of 94.68% and a robustness accuracy of 44.27%, both of which are superior to

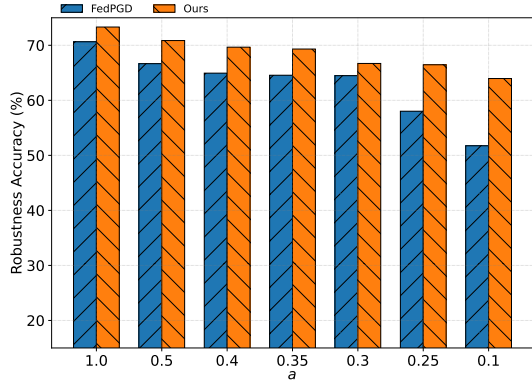


Figure 4. Robustness comparison of PM-AFL++ and FedPGD on MNIST with different levels of heterogeneities.

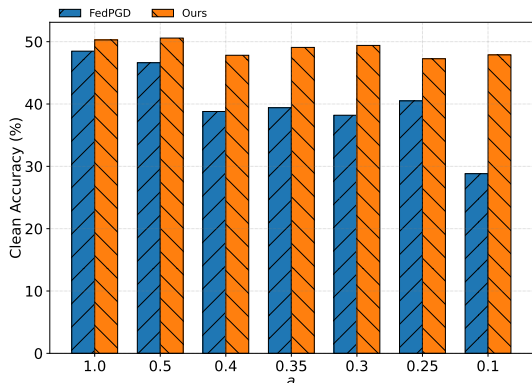


Figure 5. Accuracy comparison of PM-AFL++ and FedPGD on CIFAR-10 with different levels of heterogeneities.

or comparable with other methods. This suggests that with careful framework design, it is possible to achieve satisfactory or even superior performance with fewer communication rounds and parameters compared to larger models.

**Scalability Comparison.** Figure 4 illustrates the robustness comparison under the FGSM metric between PM-AFL++ and FedPGD. The results indicate that as the parameter  $a$  decreases, leading to higher data heterogeneity among clients, the robustness of both PM-AFL++ and FedPGD declines. However, PM-AFL++ experiences a slower decrease in robustness compared to FedPGD, highlighting its adaptability and scalability across various heterogeneity settings. Similar observations can be found in Figure 5, where we report the clean accuracy scalability comparison on CIFAR-10. It demonstrates that while both methods experience a decline in clean accuracy when data heterogeneity increases, PM-AFL++ maintains higher accuracy than FedPGD, further underscoring its effectiveness in handling varying client data distributions.

### 4.3. Ablation Study and Analysis

To thoroughly analyze the effectiveness of each module in our approach, we conduct an ablation study on the CIFAR-

Dataset	Config1	Config2	Config3	Config4	Config5	CA (%)	RA (%)
CIFAR-10	×	×	×	×	×	28.82	18.96
	✓	×	×	×	×	52.08	11.13
	✓	✓	×	×	×	57.32	8.83
	✓	✓	✓	×	×	54.06	19.65
	✓	✓	✓	✓	×	47.12	23.88
	✓	✓	✓	✓	✓	<b>47.88</b>	<b>24.03</b>
MNIST	×	×	×	×	×	91.54	21.74
	✓	×	×	×	×	92.26	2.09
	✓	✓	×	×	×	94.34	2.59
	✓	✓	✓	×	×	94.96	29.59
	✓	✓	✓	✓	×	94.40	36.41
	✓	✓	✓	✓	✓	<b>94.68</b>	<b>44.27</b>

Table 3. Ablation study of different configurations in PM-AFL++. The baseline with no configuration represents training the model from scratch using FedPGD. ‘Config1’ and ‘Config2’ denote  $loss_{vkd}^c$  and  $loss_{vkd}^f$ , respectively. ‘Config3’ and ‘Config4’ represent  $loss_{akd}^c$  and  $loss_{akd}^f$ , respectively. ‘Config5’ denotes  $loss_{cr}$ .

10 and MNIST datasets to investigate: vanilla mixture knowledge distillation (VKD), adversarial mixture knowledge distillation (AKD), and consistency regularization (CR). Quantitative results for these components are presented in Table 3. First, VKD significantly boosts CA, with CIFAR-10 showing an improvement from 28.82% to 56.78% by incorporating config 1 and config 2. However, the impact on RA is more limited, consistent with our observation in Table 1, which underscores the necessity for additional strategies to effectively mitigate adversarial attacks. The introduction of AKD (config3 and config4) leads to notable gains in robustness, as seen in CIFAR-10, where RA increases from 8.83% to 19.65% with the addition of config3, with further improvement to 23.88% when config4 is included. The final inclusion of CR (config5) enhances both clean and robust accuracy across datasets, with CIFAR-10’s CA rising from 47.12% to 47.88% and RA from 23.88% to 24.03%. Similar findings can be observed in MNIST. These results demonstrate the synergistic effect of integrating vanilla distillation, adversarial distillation, and consistency regularization, allowing PM-AFL++ to achieve superior accuracy and robustness compared to using individual components alone.

## 5. Conclusion

In this paper, we propose a novel lightweight FL framework based on mixture knowledge distillation to address the challenges of non-IID data and adversarial attacks in FL scenarios. Our method transfers both clean and adversarial prediction probabilities from a powerful teacher model to smaller local models, aiming to enhance generalization in terms of both accuracy and robustness. Furthermore, we introduce a consistency regularization term to mitigate the impact of data heterogeneity across clients. The effectiveness of our approach has been thoroughly validated against several popular baselines across various tasks.

# Pre-trained Model Guided Mixture Knowledge Distillation for Adversarial Federated Learning

## Supplementary Material

### 6. Implementation Details

#### 6.1. Pseudo Code of PM-AFL

We provide a detailed training process of the proposed algorithm, as shown in Algorithm 1. In each global round, clients receive the model parameters from the server (line 5) and then perform local training (lines 9 to 29). During local training, clients compute vanilla mixture knowledge distillation, adversarial mixture knowledge distillation, and consistency regularization in lines 20, 22, and 24, respectively. Based on these computations, clients update their model parameters (line 26) and send the updated parameters back to the server (line 29). The server then aggregates all the training parameters (line 7) and initiates the next global round until the required number of global rounds,  $T$ , is completed.

#### 6.2. Experimental Setups

Following [7, 61], we adopt CNN models as local models for the MNIST and CIFAR-10 tasks in PM-AFL. For the teacher model, we follow the approach of [62, 64] and utilize the pre-trained WideResNet-34-10 [55] and WideResNet-28-10 [55] provided by [13] as the teacher networks for CIFAR-10 and MNIST, respectively. Note that the teacher model is used locally, involves only forward propagation, and is not sent to the server for aggregation. Therefore, no additional communication costs are incurred. In contrast, for local models in other federated defense methods, we adopt larger ResNet-18 [16] and MobileNet [19] architectures for CIFAR-10 and MNIST, respectively, since these methods require training from scratch. Each local model is trained with stochastic gradient descent (SGD) using one local epoch per round, a learning rate of 0.01, a momentum of 0.9, and a weight decay of  $2e-4$ . To simulate the non-IID setting, we employ the Dirichlet distribution  $\text{Dir}(a)$ [54], where smaller values of  $a$  indicate greater skewness among clients, while larger values result in more balanced distributions. By default,  $a$  is set to 0.1. Following the recommendations in [57], we set  $\lambda = 0.2$  for MNIST and CIFAR-10. Additionally, we implement a 10-step PGD (PGD-10) with random initialization to generate adversarial examples (AEs), following the approach in [12]. For CIFAR-10, we set the perturbation bound to  $8/255$  and the step size to  $2/255$ , while for MNIST, the perturbation bound is set to 0.3 with a step size of 0.01. Final performance is evaluated by calculating the mean of the last five communication rounds, and all experimental results are av-

---

#### Algorithm 1 PM-AFL

---

##### Input:

Private dataset  $\mathcal{D}_i$  for each client, initial model parameters  $\omega$ , teacher model  $\mathcal{M}^{teacher}$ ,  $N$ , global communication rounds  $T$ .

##### Output:

Robust global model  $\omega$ .

```

1: Initialize  $\omega^0$ .
2: for  $t = 1, 2, \dots, T$  do
3:   for  $i = 0, 1, \dots, N$  in parallel do
4:     Send global model  $\omega^t$  to local client  $i$ 
5:      $\omega^t \leftarrow \text{LocalUpdate}(\omega^t)$ 
6:   end for
7:    $\mathcal{L}(\omega) \leftarrow \sum_{i \in [N]} \frac{D_i}{\sum_{i \in [N]} D_i} \mathcal{L}_i(\omega_i)$  by Eq. 2
8: end for
LocalUpdate( $\omega^t$ )
9: for each local epoch do
10:  for each batch  $(\mathbf{x}_i; y_i)$  of  $\mathcal{D}_i$  do
11:    /* Adversarial examples generation */
12:     $\mathbf{x}_i^{adv} \leftarrow \mathbf{x}_i + \delta^*$  by Eq. 5
13:    /* Clean examples augmentation */
14:     $\tilde{\mathbf{x}}_{ij} \leftarrow \lambda \mathbf{x}_i + (1 - \lambda) \mathbf{x}_j$  via Eq. 9
15:    /* Adversarial examples augmentation */
16:     $\tilde{\mathbf{x}}_{ij}^{adv} \leftarrow \lambda \mathbf{x}_i^{adv} + (1 - \lambda) \mathbf{x}_j^{adv}$  via Eq. 15
17:    Clean logits calculation for teacher and each local model via Eqs. 10 and 11, respectively.
18:    Adversarial logits calculation for each local model via Eq. 16.
19:    /* Vanilla mixture knowledge distillation */
20:     $loss_{vkd} \leftarrow loss_{vkd}^c + loss_{vkd}^f$  via Eq. 14
21:    /* Adversarial mixture knowledge distillation */
22:     $loss_{akd} \leftarrow loss_{akd}^c + loss_{akd}^f$  via Eq. 19
23:    /* Consistency regularization */
24:     $loss_{cr} \leftarrow \mathcal{L}_{cr}(z_i^{adv}, z_g)$  via Eq. 20
25:    /* Overall local objective for each client */
26:     $loss_{total} \leftarrow \gamma * loss_{vkd} + (1 - \gamma) * loss_{akd} + loss_{cr}$  via Eq. 21
27:  end for
28: end for
29: return  $\omega_i^t$ 

```

---

eraged over three independent runs. We present the adopted model architectures for CIFAR-10 and MNIST in Table 4 and Table 5, respectively.

Layer	Details
1	Conv2d(3, 128, kernel_size=3) + ReLU
2	MaxPool2d(kernel_size=2, stride=2)
3	Conv2d(128, 128, kernel_size=3) + ReLU
4	MaxPool2d(kernel_size=2, stride=2)
5	Conv2d(128, 128, kernel_size=3) + ReLU
6	Linear(128 * 4 * 4, 10)

Table 4. The model architecture used in PM-AFL for each client in the CIFAR-10 task.

Layer	Details
1	Conv2d(1, 6, kernel_size=5, stride=1) + Tanh
2	AvgPool2d(kernel_size=2)
3	Conv2d(6, 16, kernel_size=5, stride=1) + Tanh
4	AvgPool2d(kernel_size=2)
5	Conv2d(16, 120, kernel_size=4, stride=1) + Tanh
6	Linear(120, 84) + Tanh
7	Linear(84, 10)

Table 5. Model architecture used in PM-AFL for each client in the MNIST task.

## 7. Additional Results

### 7.1. Effects of Balancing Weight $\gamma$

To explore the impact of the hyperparameter  $\gamma$  in the proposed PM-AFL framework across different tasks, we define  $\rho = \frac{\gamma}{1-\gamma}$ , representing the ratio of robustness to accuracy for varying values of  $\gamma$ . The robustness evaluation results for CIFAR-10 are presented in Figure 6. For a comprehensive assessment, robustness is evaluated against a diverse range of adversarial attacks, including FGSM, BIM, PGD-40, PGD-100, Square, and AA attacks. The results indicate that as the ratio  $\rho$  increases, robustness rises rapidly, reaching a plateau after  $\rho = 3.0/1.0$ . Beyond this point, when  $\rho$  exceeds 3.0/1.0, robustness fluctuates slightly, with optimal performance observed at  $\rho = 5.0/1.0$ . Similarly, we also report the robustness evaluation results for MNIST in Figure 7. The best performance is observed at  $\rho = 5.0/1.0$ .

### 7.2. Effects of Temperature $T$

The temperature  $T$  is used to control the smoothness of the distillation process, with larger values of  $T$  producing smoother class probabilities and allowing more information to be distilled. We evaluate the impact of  $T$  on the performance of PM-AFL in Table 6. The results indicate that PM-AFL achieves optimal trade-off performance with  $T = 3$  for

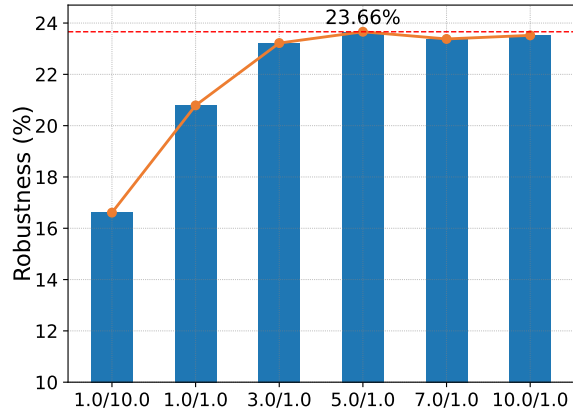


Figure 6. **Robustness of PM-AFL on CIFAR-10 under different values of  $\rho$ .** The X-axis represents the ratio of robustness to accuracy, defined as  $\rho = \frac{\gamma}{1-\gamma}$ . The Y-axis illustrates robustness against a diverse range of attacks. The selected value of  $\rho$  is 5.0/1.0.

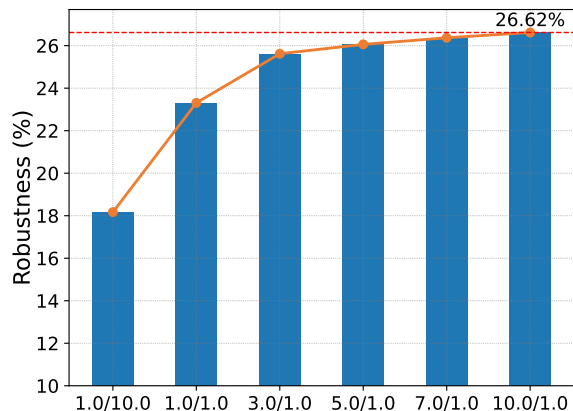


Figure 7. **Robustness of PM-AFL on MNIST under different values of  $\rho$ .** The X-axis represents the ratio of robustness to accuracy, defined as  $\rho = \frac{\gamma}{1-\gamma}$ . The Y-axis illustrates robustness against a diverse range of attacks. The selected value of  $\rho$  is 10.0/1.0.

Dataset	MNIST		Cifar-10	
	Acc.	Rob.	Acc.	Rob.
1.0	92.58	26.62	43.52	23.66
2.0	94.62	41.87	<b>47.88</b>	<b>24.03</b>
3.0	<b>94.68</b>	<b>44.27</b>	47.08	23.25
4.0	94.28	43.45	46.82	23.08
5.0	94.22	41.95	47.37	23.01

Table 6. Effect of hyper-parameter  $T$ . ‘‘Acc.’’ refers to the clean accuracy (%), while ‘‘Rob.’’ denotes the robustness (%) against six attacks.

MNIST and  $T = 2$  for CIFAR-10.

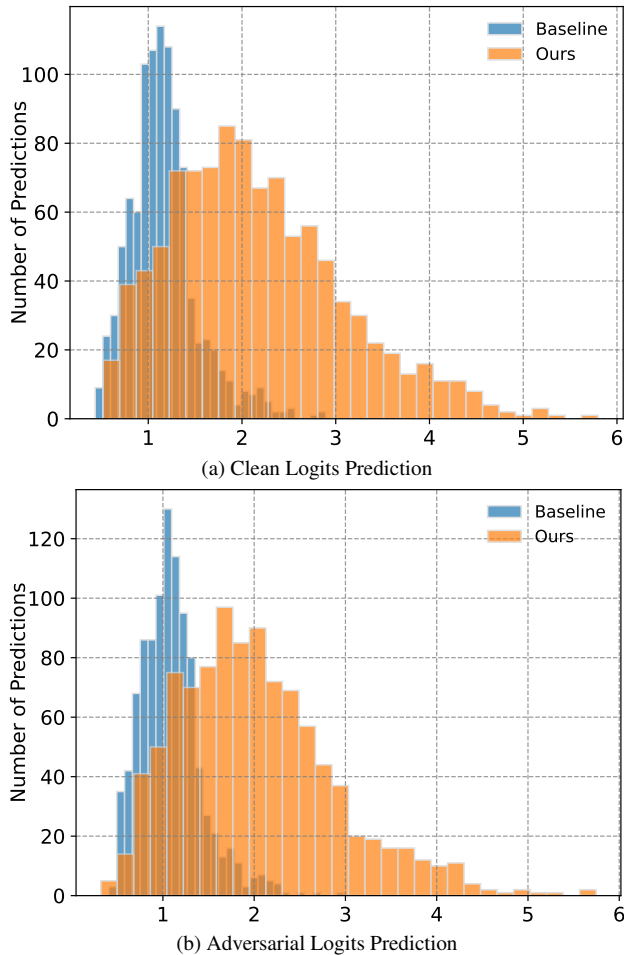


Figure 8. **Logits Prediction Values Comparison on CIFAR-10.** The X-axis represents the predicted logits values, and the Y-axis illustrates the number of predictions. The adversarial logits predictions are measured under PGD-40 attacks.

### 7.3. Logits Prediction Visualization and Discussion

Figure 8 presents the logits distributions for both our model and the baseline, providing insight into the effectiveness of our approach. Since FedPGD is a direct robust extension of FedAvg, we use it as the baseline for comparison. Both models are trained on the CIFAR-10 dataset using a CNN model with the default Dirichlet distribution, with the baseline model trained from scratch using this architecture. From the results, we make the following observations. First, compared to the baseline, our method demonstrates a broader distribution in both clean and adversarial logit predictions. This may suggest that our training approach can enable the model to achieve more balanced predictions. Second, we observe that the baseline is concentrated at lower logit values, whereas our logits are distributed in a higher value range. This distinction highlights the relatively stronger prediction confidence than the base-

line. Overall, these differences indicate that our approach might not only achieve more balanced predictions but also enhance prediction confidence.

### 7.4. Further Explorations

**How Do Baselines Perform With the Same Local Model as PM-AFL?** While PM-AFL aims to leverage the teacher model to guide each local model, it remains unclear whether training a baseline from scratch using the same local model as PM-AFL would result in better performance. To explore this, we train all baselines from scratch using the same model architecture as PM-AFL, with the results presented in Table 7. The results indicate that PM-AFL consistently outperforms several baselines, even with fewer communication rounds. For instance, on the CIFAR-10 dataset, FedPGD achieves 26.42% clean accuracy and 18.72% averaged adversarial robustness, while PM-AFL significantly improves these metrics to 47.88% clean accuracy and 24.03% adversarial robustness. These results further underscore the superiority of knowledge-distillation-based methods over training from scratch.

**A Larger Model Can Benefit the Baselines More?** To further investigate the impact of different model sizes on performance, we evaluate the baselines using various local models. As in the previous analysis, we adopt the FedPGD method as the baseline to assess performance across different local models. Following most studies [14, 21, 56] that perform robustness analysis on CIFAR-10, we also conduct experiments on this dataset, with the results reported in Table 8. From the results, we observe that increasing the model size from CNN to ResNet10 or ResNet12 leads to improvements in both clean accuracy and adversarial robustness. However, as the model size continues to grow with architectures like ResNet18 and WideResNet-34-10 (WRN-34-10), performance declines across both metrics. For instance, scaling from ResNet18 to WRN-34-10 increases the number of parameters by approximately four times, yet both clean accuracy and adversarial robustness remain nearly unchanged. Specifically, the clean accuracy reaches 28.82% for ResNet18 but drops to 27.92% for WRN-34-10. In contrast, despite the CNN model having 150 times fewer parameters than WRN-34-10, it achieves comparable performance, highlighting that training a large model from scratch in adversarial federated learning may not necessarily yield better results.

**A Larger Model Can Inherit More Performance From the Teacher?** In knowledge distillation, the capacity of the student model plays a crucial role in determining how effectively it can absorb knowledge from the teacher [17]. This raises an important question: does increasing the model size lead to better performance gains when inheriting knowledge from the teacher in adversarial federated learning? To explore this, we conduct experiments using

Dataset	Method	Clean Acc.	Robust Acc.						# of Comm Rounds	
			FGSM	BIM	PGD-40	PGD-100	Square	AA		Avg
CIFAR-10	FedAvg [33]	45.26	7.62	5.40	5.42	5.35	6.50	4.28	5.76	200
	MixFAT [65]	31.88	20.32	19.52	19.62	19.60	18.28	17.32	19.11	250
	FedPGD [32]	26.42	19.74	18.96	19.00	18.98	18.16	17.48	18.72	200
	FedALP [23]	25.60	18.74	18.38	18.36	18.32	17.12	16.56	17.91	200
	FedMART [48]	28.18	20.52	19.60	19.62	19.60	18.44	17.74	19.25	200
	FedTRADES [59]	29.76	20.64	19.66	19.70	19.66	18.02	16.92	19.10	230
	CalFAT [7]	26.02	18.64	17.98	17.96	17.94	17.16	16.64	17.72	200
	DBFAT [61]	33.44	21.50	20.88	20.94	20.90	18.70	17.56	20.08	200
	<b>PM-AFL</b>	45.76	24.46	23.96	22.96	22.94	21.26	18.74	22.38	150
	<b>PM-AFL++</b>	<b>47.88</b>	<b>26.80</b>	<b>24.62</b>	<b>24.68</b>	<b>24.66</b>	<b>23.20</b>	<b>20.22</b>	<b>24.03</b>	<b>150</b>
MNIST	FedAvg [33]	92.22	1.28	4.14	0.00	0.00	0.00	0.00	0.90	160
	MixFAT [65]	88.12	14.92	44.76	6.92	4.02	3.94	2.98	12.92	160
	FedPGD [32]	87.98	16.06	47.42	7.72	4.30	4.56	3.14	13.86	160
	FedALP [23]	86.24	24.68	52.52	13.54	8.84	8.08	6.32	18.99	180
	FedMART [48]	85.04	22.72	51.32	13.08	9.36	7.36	6.08	18.32	160
	FedTRADES [59]	89.96	27.02	55.96	13.34	8.16	8.36	6.26	19.85	160
	CalFAT [7]	88.64	20.52	51.20	10.14	5.78	5.94	4.16	16.29	180
	DBFAT [61]	91.24	37.20	62.14	18.74	10.48	10.20	8.20	24.49	180
	<b>PM-AFL</b>	94.53	57.89	72.15	33.41	18.72	17.84	13.66	35.61	100
	<b>PM-AFL++</b>	<b>94.68</b>	<b>63.96</b>	<b>77.50</b>	<b>43.10</b>	<b>29.92</b>	<b>27.52</b>	<b>23.62</b>	<b>44.27</b>	<b>100</b>

Table 7. Comparison of different methods on benchmark datasets under non-IID data using the same model architecture for local models. The best results are in **bold**. PM-AFL appears to outperform the baselines, achieving higher accuracy (%) and robustness (%) while requiring fewer communication rounds.

Model	Clean Acc. (%)	AA Acc. (%)	# of Comm Params ( $\times 10^3$ )
CNN	26.42	17.48	320
ResNet10	33.28	19.24	4,903
ResNet12	30.18	17.74	4,977
ResNet18	28.82	17.22	11,690
ResNet20	27.52	16.84	17,297
ResNet34	25.02	16.10	21,282
WRN-34-10	27.92	16.42	48,263

Table 8. Comparison of different model architectures used in FedPGD on CIFAR-10 dataset under non-IID data. “WRN-34-10” refers to the WideResNet-34-10 model. All methods are conducted over 200 global iterations.

Model	Clean Acc. (%)	AA Acc. (%)	# of Comm Params ( $\times 10^3$ )
CNN	50.06	20.28	320
ResNet10	57.98	24.66	4,903
ResNet12	58.12	25.40	4,977
ResNet18	57.22	25.72	11,690
ResNet20	55.28	24.90	17,297
ResNet34	55.68	24.76	21,282
WRN-34-10	55.94	24.78	48,263

Table 9. Comparison of different model architectures used in **PM-AFL** on CIFAR-10 dataset under non-IID data. “WRN-34-10” refers to the WideResNet-34-10 model. All methods are conducted over 200 global iterations.

various model architectures, as shown in Table 9. The results suggest that our approach can benefit from larger model sizes. For instance, using ResNet10 for distillation leads to higher clean accuracy and adversarial robustness compared to smaller models like CNN. However, the performance improvement does not scale linearly with model size. While ResNet12 achieves slightly better adversarial accuracy than ResNet10, the significantly larger WRN-34-10 only offers marginal gains over ResNet18 in both clean and adversarial accuracy. This suggests that while increasing model size can enhance the student model’s ability to absorb knowledge, it may not always be necessary to select a larger model. A moderately sized student model can still achieve effective distillation, offering a balance between performance and model complexity.

## References

- [1] Maksym Andriushchenko, Francesco Croce, Nicolas Flammarion, and Matthias Hein. Square attack: a query-efficient black-box adversarial attack via random search. In *European Conference on Computer Vision*, pages 484–501, Glasgow, UK, 2020. Springer. 3, 7
- [2] Rodolfo Stoffel Antunes, Cristiano André da Costa, Arne Küderle, Imrana Abdullahi Yari, and Björn Eskofier. Federated learning for healthcare: Systematic review and architecture proposal. *ACM Transactions on Intelligent Systems and Technology (TIST)*, 13(4):1–23, 2022. 1

- [3] Anish Athalye and Nicholas Carlini. On the robustness of the cvpr 2018 white-box adversarial example defenses. In *The Bright and Dark Sides of Computer Vision: Challenges and Opportunities for Privacy and Security*, 2018. 4
- [4] Narayanaswamy Balakrishnan. Continuous multivariate distributions. *Wiley StatsRef: Statistics Reference Online*, 2014. 3
- [5] Lucas Beyer, Xiaohua Zhai, Amélie Royer, Larisa Markeeva, Rohan Anil, and Alexander Kolesnikov. Knowledge distillation: A good teacher is patient and consistent. In *Proceedings of the IEEE/CVF conference on computer vision and pattern recognition*, pages 10925–10934, 2022. 2
- [6] Nicholas Carlini and David Wagner. Towards evaluating the robustness of neural networks. In *2017 IEEE Symposium on Security and Privacy (SP)*, pages 39–57. IEEE, 2017. 3
- [7] Chen Chen, Yuchen Liu, Xingjun Ma, and Lingjuan Lyu. Calfat: Calibrated federated adversarial training with label skewness. *Advances in Neural Information Processing Systems*, 35:3569–3581, 2022. 2, 3, 4, 6, 7, 1
- [8] Hongjun Choi, Eun Som Jeon, Ankita Shukla, and Pavan Turaga. Understanding the role of mixup in knowledge distillation: An empirical study. In *Proceedings of the IEEE/CVF Winter Conference on Applications of Computer Vision*, pages 2319–2328, 2023. 2
- [9] Francesco Croce and Matthias Hein. Reliable evaluation of adversarial robustness with an ensemble of diverse parameter-free attacks. In *International conference on machine learning*, pages 2206–2216. PMLR, 2020. 3, 7
- [10] Gongfan Fang, Jie Song, Chengchao Shen, Xinchao Wang, Da Chen, and Mingli Song. Data-free adversarial distillation. *arXiv preprint arXiv:1912.11006*, 2019. 3
- [11] Micah Goldblum, Liam Fowl, Soheil Feizi, and Tom Goldstein. Adversarially robust distillation. In *Proceedings of the AAAI conference on artificial intelligence*, pages 3996–4003, NY, USA, 2020. 2, 3
- [12] Ian J Goodfellow, Jonathon Shlens, and Christian Szegedy. Explaining and harnessing adversarial examples. In *International Conference on Learning Representations*, CA, USA, 2015. 1, 3, 7
- [13] Sven Gowal, Chongli Qin, Jonathan Uesato, Timothy Mann, and Pushmeet Kohli. Uncovering the limits of adversarial training against norm-bounded adversarial examples. *arXiv preprint arXiv:2010.03593*, 2020. 1
- [14] Sven Gowal, Sylvestre-Alvise Rebuffi, Olivia Wiles, Florian Stimberg, Dan Andrei Calian, and Timothy A Mann. Improving robustness using generated data. *Advances in Neural Information Processing Systems*, 34:4218–4233, 2021. 3
- [15] Yushuo Guan, Pengyu Zhao, Bingxuan Wang, Yuanxing Zhang, Cong Yao, Kaigui Bian, and Jian Tang. Differentiable feature aggregation search for knowledge distillation. In *Computer Vision—ECCV 2020: 16th European Conference, Glasgow, UK, August 23–28, 2020, Proceedings, Part XVII 16*, pages 469–484, Glasgow, UK, 2020. Springer. 3
- [16] Kaiming He, Xiangyu Zhang, Shaoqing Ren, and Jian Sun. Deep residual learning for image recognition. In *Proceedings of the IEEE conference on computer vision and pattern recognition*, pages 770–778, 2016. 7, 1
- [17] Geoffrey Hinton, Oriol Vinyals, and Jeff Dean. Distilling the knowledge in a neural network. *arXiv preprint arXiv:1503.02531*, 2015. 2, 3, 4
- [18] Junyuan Hong, Haotao Wang, Zhangyang Wang, and Jiayu Zhou. Federated robustness propagation: sharing adversarial robustness in heterogeneous federated learning. In *Proceedings of the AAAI Conference on Artificial Intelligence*, pages 7893–7901, WA., USA, 2023. 1, 3, 4
- [19] Andrew G Howard, Menglong Zhu, Bo Chen, Dmitry Kalenichenko, Weijun Wang, Tobias Weyand, Marco Andreetto, and Hartwig Adam. Mobilenets: Efficient convolutional neural networks for mobile vision applications. *arXiv preprint arXiv:1704.04861*, 2017. 7, 1
- [20] Tzu-Ming Harry Hsu, Hang Qi, and Matthew Brown. Measuring the effects of non-identical data distribution for federated visual classification. *arXiv preprint arXiv:1909.06335*, 2019. 2
- [21] Shihua Huang, Zhichao Lu, Kalyanmoy Deb, and Vishnu Naresh Boddeti. Revisiting residual networks for adversarial robustness. In *Proceedings of the IEEE/CVF Conference on Computer Vision and Pattern Recognition*, pages 8202–8211, 2023. 3
- [22] Wenke Huang, Mang Ye, Zekun Shi, He Li, and Bo Du. Rethinking federated learning with domain shift: A prototype view. In *2023 IEEE/CVF Conference on Computer Vision and Pattern Recognition (CVPR)*, pages 16312–16322. IEEE, 2023. 2
- [23] Harini Kannan, Alexey Kurakin, and Ian Goodfellow. Adversarial logit pairing. *arXiv preprint arXiv:1803.06373*, 2018. 6, 7, 4
- [24] Alex Krizhevsky, Geoffrey Hinton, et al. Learning multiple layers of features from tiny images. *Toronto, ON, Canada*, pages 32–33, 2009. 6
- [25] Alexey Kurakin, Ian J Goodfellow, and Samy Bengio. Adversarial examples in the physical world. In *Artificial Intelligence Safety and Security*, pages 99–112. Chapman and Hall/CRC, 2018. 3, 7
- [26] Yann LeCun, Léon Bottou, Yoshua Bengio, and Patrick Haffner. Gradient-based learning applied to document recognition. *Proceedings of the IEEE*, 86(11):2278–2324, 1998. 6
- [27] Qinbin Li, Bingsheng He, and Dawn Song. Model-contrastive federated learning. In *Proceedings of the IEEE/CVF Conference on Computer Vision and Pattern Recognition*, pages 10713–10722, TN, USA, 2021. 2
- [28] Tian Li, Anit Kumar Sahu, Manzil Zaheer, Maziar Sanjabi, Ameet Talwalkar, and Virginia Smith. Federated optimization in heterogeneous networks. *Proceedings of Machine learning and systems*, 2:429–450, 2020. 2
- [29] Tao Lin, Lingjing Kong, Sebastian U Stich, and Martin Jaggi. Ensemble distillation for robust model fusion in federated learning. *Advances in Neural Information Processing Systems*, 33:2351–2363, 2020. 3
- [30] Guodong Long, Yue Tan, Jing Jiang, and Chengqi Zhang. Federated learning for open banking. In *Federated learning: privacy and incentive*, pages 240–254. Springer, 2020. 1

- [31] Zihao Lu, Junli Wang, and Changjun Jiang. Data-free knowledge filtering and distillation in federated learning. *IEEE Transactions on Big Data*, 2024. 3
- [32] Aleksander Madry, Aleksandar Makelov, Ludwig Schmidt, Dimitris Tsipras, and Adrian Vladu. Towards deep learning models resistant to adversarial attacks. In *International Conference on Learning Representations*, BC, Canada, 2018. 3, 6, 7, 4
- [33] Brendan McMahan, Eider Moore, Daniel Ramage, Seth Hampson, and Blaise Aguera y Arcas. Communication-efficient learning of deep networks from decentralized data. In *Artificial Intelligence and Statistics*, pages 1273–1282. PMLR, 2017. 1, 2, 3, 7, 4
- [34] Seyed-Mohsen Moosavi-Dezfooli, Alhussein Fawzi, Omar Fawzi, and Pascal Frossard. Universal adversarial perturbations. In *Proceedings of the IEEE conference on computer vision and pattern recognition*, pages 1765–1773, 2017. 3
- [35] Nikolaos Passalis, Maria Tzelepi, and Anastasios Tefas. Probabilistic knowledge transfer for lightweight deep representation learning. *IEEE Transactions on Neural Networks and Learning Systems*, 32(5):2030–2039, 2020. 3
- [36] Yu Qiao, Chaoning Zhang, Taegoo Kang, Donghun Kim, Shehbaz Tariq, Chenshuang Zhang, and Choong Seon Hong. Robustness of sam: Segment anything under corruptions and beyond. *arXiv preprint arXiv:2306.07713*, 2023. 3
- [37] Yu Qiao, Apurba Adhikary, Chaoning Zhang, and Choong Seon Hong. Towards robust federated learning via logits calibration on non-iid data. In *NOMS 2024-2024 IEEE/IFIP Network Operations and Management Symposium*, Seoul, Korea, 2024. IEEE. 2, 3
- [38] Yu Qiao, Md Shirajum Munir, Apurba Adhikary, Huy Q Le, Avi Deb Raha, Chaoning Zhang, and Choong Seon Hong. Mp-fedcl: Multiprototype federated contrastive learning for edge intelligence. *IEEE Internet of Things Journal*, 11(5):8604–8623, 2024. 1
- [39] Yu Qiao, Chaoning Zhang, Apurba Adhikary, and Choong Seon Hong. Logit calibration and feature contrast for robust federated learning on non-iid data. *IEEE Transactions on Network Science and Engineering*, 2024. 1, 2, 3, 4
- [40] Yu Qiao, Huy Q Le, Mengchun Zhang, Apurba Adhikary, Chaoning Zhang, and Choong Seon Hong. Fedccl: Federated dual-clustered feature contrast under domain heterogeneity. *Information Fusion*, 113:102645, 2025. 2
- [41] Sara Salim, Nour Moustafa, Benjamin Turnbull, and Imran Razzak. Perturbation-enabled deep federated learning for preserving internet of things-based social networks. *ACM Transactions on Multimedia Computing, Communications, and Applications (TOMM)*, 18(2s):1–19, 2022. 1
- [42] Shangquan Sun, Wenqi Ren, Jingzhi Li, Rui Wang, and Xiaochun Cao. Logit standardization in knowledge distillation. In *Proceedings of the IEEE/CVF Conference on Computer Vision and Pattern Recognition*, pages 15731–15740, WA, USA, 2024. 3
- [43] Christian Szegedy, Wojciech Zaremba, Ilya Sutskever, Joan Bruna, Dumitru Erhan, Ian Goodfellow, and Rob Fergus. Intriguing properties of neural networks. *arXiv preprint arXiv:1312.6199*, 2013. 1, 3, 4
- [44] Canh T Dinh, Nguyen Tran, and Josh Nguyen. Personalized federated learning with moreau envelopes. *Advances in Neural Information Processing Systems*, 33:21394–21405, 2020. 2
- [45] Yue Tan, Guodong Long, Lu Liu, Tianyi Zhou, Qinghua Lu, Jing Jiang, and Chengqi Zhang. Fedproto: Federated prototype learning across heterogeneous clients. In *Proceedings of the AAAI Conference on Artificial Intelligence*, pages 8432–8440, 2022. 2
- [46] Ningfei Wang, Yunpeng Luo, Takami Sato, Kaidi Xu, and Qi Alfred Chen. Does physical adversarial example really matter to autonomous driving? towards system-level effect of adversarial object evasion attack. In *Proceedings of the IEEE/CVF International Conference on Computer Vision*, pages 4412–4423, 2023. 3
- [47] Shuai Wang, Yexuan Fu, Xiang Li, Yunshi Lan, Ming Gao, et al. Dfdr: Data-free robustness distillation for heterogeneous federated learning. *Advances in Neural Information Processing Systems*, 36, 2024. 3
- [48] Yisen Wang, Difan Zou, Jinfeng Yi, James Bailey, Xingjun Ma, and Quanquan Gu. Improving adversarial robustness requires revisiting misclassified examples. In *International conference on learning representations*, 2019. 6, 7, 4
- [49] Yuan Wang, Huazhu Fu, Renuga Kanagavelu, Qingsong Wei, Yong Liu, and Rick Siow Mong Goh. An aggregation-free federated learning for tackling data heterogeneity. In *Proceedings of the IEEE/CVF Conference on Computer Vision and Pattern Recognition*, pages 26233–26242, WA, USA, 2024. 3
- [50] Yi Xie, Hanxiao Wu, Yihong Lin, Jianqing Zhu, and Huanqiang Zeng. Pairwise difference relational distillation for object re-identification. *Pattern Recognition*, 152:110455, 2024. 3
- [51] Yunlu Yan, Chun-Mei Feng, Mang Ye, Wangmeng Zuo, Ping Li, Rick Siow Mong Goh, Lei Zhu, and CL Chen. Rethinking client drift in federated learning: A logit perspective. *arXiv preprint arXiv:2308.10162*, 2023. 3
- [52] Shikang Yu, Jiachen Chen, Hu Han, and Shuqiang Jiang. Data-free knowledge distillation via feature exchange and activation region constraint. In *Proceedings of the IEEE/CVF Conference on Computer Vision and Pattern Recognition*, pages 24266–24275, Vancouver, Canada, 2023. 3
- [53] Li Yuan, Francis EH Tay, Guilin Li, Tao Wang, and Jiashi Feng. Revisiting knowledge distillation via label smoothing regularization. In *Proceedings of the IEEE/CVF conference on computer vision and pattern recognition*, pages 3903–3911, 2020. 2
- [54] Mikhail Yurochkin, Mayank Agarwal, Soumya Ghosh, Kristjan Greenewald, Nghia Hoang, and Yasaman Khazani. Bayesian nonparametric federated learning of neural networks. In *International Conference on Machine Learning*, pages 7252–7261, CA, USA, 2019. PMLR. 3, 7, 1
- [55] Sergey Zagoruyko. Wide residual networks. *arXiv preprint arXiv:1605.07146*, 2016. 7, 1
- [56] Chenshuang Zhang, Chaoning Zhang, Kang Zhang, Axi Niu, Junmo Kim, and In So Kweon. Towards understanding dual bn in hybrid adversarial training. *arXiv preprint arXiv:2403.19150*, 2024. 3

- [57] Hongyi Zhang, Moustapha Cisse, Yann N Dauphin, and David Lopez-Paz. mixup: Beyond empirical risk minimization. *arXiv preprint arXiv:1710.09412*, 2017. [2](#), [5](#), [6](#), [7](#), [1](#)
- [58] Huan Zhang, Hongge Chen, Zhao Song, Duane Boning, Inderjit Dhillon, and Cho Jui Hsieh. The limitations of adversarial training and the blind-spot attack. In *7th International Conference on Learning Representations, ICLR 2019, LA, USA, 2019*. [3](#)
- [59] Hongyang Zhang, Yaodong Yu, Jiantao Jiao, Eric Xing, Laurent El Ghaoui, and Michael Jordan. Theoretically principled trade-off between robustness and accuracy. In *International Conference on Machine Learning*, pages 7472–7482, CA, USA, 2019. PMLR. [6](#), [7](#), [4](#)
- [60] Jie Zhang, Zhiqi Li, Bo Li, Jianghe Xu, Shuang Wu, Shouhong Ding, and Chao Wu. Federated learning with label distribution skew via logits calibration. In *International Conference on Machine Learning*, pages 26311–26329. PMLR, 2022. [3](#)
- [61] Jie Zhang, Bo Li, Chen Chen, Lingjuan Lyu, Shuang Wu, Shouhong Ding, and Chao Wu. Delving into the adversarial robustness of federated learning. In *Proceedings of the AAAI Conference on Artificial Intelligence*, pages 11245–11253, DC, USA, 2023. [1](#), [2](#), [3](#), [4](#), [6](#), [7](#)
- [62] Shiji Zhao, Jie Yu, Zhenlong Sun, Bo Zhang, and Xingxing Wei. Enhanced accuracy and robustness via multi-teacher adversarial distillation. In *European Conference on Computer Vision*, pages 585–602. Springer, 2022. [1](#)
- [63] Zhuangdi Zhu, Junyuan Hong, and Jiayu Zhou. Data-free knowledge distillation for heterogeneous federated learning. In *International conference on machine learning*, pages 12878–12889. PMLR, 2021. [3](#)
- [64] Bojia Zi, Shihao Zhao, Xingjun Ma, and Yu-Gang Jiang. Revisiting adversarial robustness distillation: Robust soft labels make student better. In *Proceedings of the IEEE/CVF International Conference on Computer Vision*, pages 16443–16452, 2021. [2](#), [1](#)
- [65] Giulio Zizzo, Amrbrish Rawat, Mathieu Sinn, and Beat Buesser. Fat: Federated adversarial training. In *Annual Conference on Neural Information Processing Systems*, 2020. [1](#), [3](#), [6](#), [7](#), [4](#)